








ORIGINAL RESEARCH

Angiotensin II Induces Aortic Rupture and Dissection in Osteoprotegerin-Deficient Mice

Toshihiro Tsuruda , MD, PhD; Atsushi Yamashita , MD, PhD; Misa Otsu, BNS; Masanori Koide , DDS, PhD; Yuko Nakamichi , PhD; Yoko Sekita-Hatakeyama , PhD; Kinta Hatakeyama , MD, PhD; Taro Funamoto, MD, PhD; Etsuo Chosa, MD, PhD; Yujiro Asada , MD, PhD; Nobuyuki Udagawa, DDS, PhD; Johji Kato, MD, PhD; Kazuo Kitamura, MD, PhD

BACKGROUND: The biological mechanism of action for osteoprotegerin, a soluble decoy receptor for the receptor activator of nuclear factor-kappa B ligand in the vascular structure, has not been elucidated. The study aim was to determine if osteoprotegerin affects aortic structural integrity in angiotensin II (Ang II)-induced hypertension.

METHODS AND RESULTS: Mortality was higher ($P<0.0001$ by log-rank test) in 8-week-old male homozygotes of osteoprotegerin gene-knockout mice given subcutaneous administration of Ang II for 28 days, with an incidence of 21% fatal aortic rupture and 23% aortic dissection, than in age-matched wild-type mice. Ang II-infused aorta of wild-type mice showed that osteoprotegerin immunoreactivity was present with proteoglycan. The absence of osteoprotegerin was associated with decreased medial and adventitial thickness and increased numbers of elastin breaks as well as with increased periostin expression and soluble receptor activator of nuclear factor-kappa B ligand concentrations. PEGylated human recombinant osteoprotegerin administration decreased all-cause mortality ($P<0.001$ by log-rank test), the incidence of fatal aortic rupture ($P=0.08$), and aortic dissection ($P<0.001$) with decreasing numbers of elastin breaks, periostin expressions, and soluble receptor activator of nuclear factor-kappa B ligand concentrations in Ang II-infused osteoprotegerin gene-knockout mice.

CONCLUSIONS: These data suggest that osteoprotegerin protects against aortic rupture and dissection in Ang II-induced hypertension by inhibiting receptor activator of nuclear factor-kappa B ligand activity and periostin expression.

Key Words: aortic dissection ■ elastin ■ extracellular matrix ■ proteoglycan

Aortic dissection occurs at a rate of 3.5 to 5 per 100 000 annually^{1,2} and has a high in-hospital overall mortality rate (22% for type A versus 14% for type B).³ Hypertension is the most important risk factor for increasing the incidence of aortic dissection after adjusting for age and sex.² Fragmentation of elastic fibers and reduction in numbers of smooth muscle cells accompanied by an accumulation of proteoglycans are observed in dissected human aorta.⁴ Matrix metalloproteinases degrade elastic fibers that endow the aortic wall with resilience and collagen fibers that

endow the wall strength.⁵ Proteoglycans with negatively charged glycosaminoglycan generate an interstitial swelling pressure that may be mechanically disruptive to fibrillar proteins.⁶ In addition, the numbers of heparin-binding proteins binding to glycosaminoglycan might be sufficient to affect disease progression.⁷⁻⁹ However, it remains unknown which molecules binding to them might help initiate aortic rupture and dissection.

Osteoprotegerin is a soluble glycoprotein belonging to the tumor necrosis factor receptor superfamily and consists of 380 amino acids containing 7 domains:

Correspondence to: Toshihiro Tsuruda, MD, PhD, Cardiorenal Research Laboratory, Department of Hemo-Vascular Advanced Medicine, Faculty of Medicine, University of Miyazaki, Miyazaki 889-1692, Japan. Email: ttsuruda@med.miyazaki-u.ac.jp

Supplemental Material is available at <https://www.ahajournals.org/doi/suppl/10.1161/JAHA.122.025336>

For Sources of Funding and Disclosures, see page 10.

© 2022 The Authors. Published on behalf of the American Heart Association, Inc., by Wiley. This is an open access article under the terms of the Creative Commons Attribution-NonCommercial-NoDerivs License, which permits use and distribution in any medium, provided the original work is properly cited, the use is non-commercial and no modifications or adaptations are made.

JAHA is available at: www.ahajournals.org/journal/jaha

CLINICAL PERSPECTIVE

What Is New?

- This study demonstrates that the osteoprotegerin–proteoglycan complex might contribute to the pathogenesis of aortic rupture and dissection and that the complex may be associated with the inhibition of receptor activator of nuclear factor-kappa B ligand activity and periostin expression.

What Are the Clinical Implications?

- The supplementation of osteoprotegerin could be useful for decreasing the risk of aortic rupture and dissection.

Nonstandard Abbreviations and Acronyms

Ang II	angiotensin II
RANKL	receptor activator of nuclear factor-kappa B ligand

4 cysteine-rich N-terminal domains (domains 1–4), 2 death-domain homologous regions (domains 5 and 6), and a C-terminal heparin-binding domain (domain 7).¹⁰ Osteoprotegerin works as a decoy receptor for the receptor activator of nuclear factor-kappa B ligand (RANKL) through domains 1 to 4 to inhibit binding to its receptor RANK, leading to regulation of osteoclasts maturation.^{11,12} RANKL is mainly released from bone and primary/secondary lymphoid organs. Osteoprotegerin and RANK are widely distributed in vascular walls.^{13–16} Deletion or loss of function of the osteoprotegerin gene leads to marked activation of RANKL signaling, which results in a deformity of bone condition from childhood named juvenile Paget disease.¹⁷ Some patients with this disorder show giant bilateral cavernous carotid artery aneurysms and angiod streaks by breaking the elastic fibers.^{18,19} We hypothesized that osteoprotegerin not only regulates bone metabolism but also has a role in maintaining the structural integrity of vascular walls. To test our hypothesis, we administered a vasoconstrictive peptide, angiotensin II (Ang II), to the wild-type (WT) and homozygotes of osteoprotegerin gene-knockout (OPG^{-/-}) mice to explore the pathological roles of osteoprotegerin in the vasculature.

METHODS

Ethical Considerations

All protocols for the animal experiments were reviewed and approved by the University of the Miyazaki

Institutional Animal Care and Use Committee (approval number 2018-516) and Genetic Modification Safety Committee of Miyazaki University (approval number 600). All studies were conducted in accordance with the National Institute of Health *Guide for the Care and Use of Laboratory Animals* (Revised 2015). The data that support the findings of this study are available from the corresponding author upon reasonable request.

Animal Experiments

Mice were housed in a temperature- and light-controlled room (25°C±1°C; 12/12-hour light/dark cycle) with free access to normal chow and water. OPG^{-/-} mice (genetic background of C57BL/6) were generated by targeted disruption of the gene,²⁰ and OPG^{-/-} mice were bred with OPG^{-/-} mice. WT mice (C57BL/6J) were purchased from Japan Clea Co. (Tokyo, Japan). The phenotype of each mouse was verified at every mating by polymerase chain reaction analysis of the tail DNA. Eight-week-old male OPG^{-/-} mice and age-matched WT mice (Japan Clea Co.) were used in this study. OPG^{-/-} and age-matched WT mice were anesthetized by injecting 0.75 mg/kg medetomidine, 4 mg/kg midazolam, and 5 mg/kg butorphanol intraperitoneally. Either Ang II (1000 ng/kg per minute dissolved in 0.9% saline) or vehicle (0.9% saline) was infused subcutaneously for 28 days by using the implanted mini-osmotic pump (Alzet, Model 1004; DURECT Co.). In another setting of experiments, 10 mg/kg of human recombinant osteoprotegerin (hrOPG)/osteoclastogenesis inhibitory factor, which was (poly)PEGylated at the C-terminus region to interact with heparin sulfate proteoglycan, dissolved in 10 mmol/L Na-Pi, 0.15 mol/L NaCl, and 0.01% polysorbate 80 (pH 7.4) (provided by Daiichi-Sankyo Co., Ltd, Tokyo, Japan)²¹ was administered intraperitoneally to the Ang II-infused OPG^{-/-} mice every 2 days from day 1 to 28. At day 28, we anesthetized the mice by injecting 0.75 mg/kg medetomidine, 4 mg/kg midazolam, and 5 mg/kg butorphanol intraperitoneally and removed the aorta. If the mice died during the experimental periods, we performed a necropsy to determine a possible cause of death. A finding of blood clots in the chest or abdominal cavity was judged to be aortic rupture, and transparent effusion in the chest cavity was judged to be heart failure. We defined aortic dissection in survived mice as the presence of blood clots microscopically in the false lumen.

Sample Collection

Blood

At day 28, blood samples were collected from the left ventricle of mice under anesthesia and mixed with 10 µL of 10 mg/mL EDTA-2Na and 0.7 mg/mL aprotinin. The mixture was centrifuged at 830g at 4°C for 10 minutes. The plasma was then stored at -80°C until use.

Aorta

The mice aortae were harvested from the aortic arch to the common iliac artery bifurcation by perfusion fixation with 4% paraformaldehyde, followed by immersion in 4% paraformaldehyde overnight for the histological analysis, or perfused with phosphate-buffered saline and immersed in RNAlater (Ambion) at 4°C overnight for polymerase chain reaction (PCR) array analysis.

Blood Pressure

Systolic blood pressure was measured 3 times by tail-cuff plethysmography (BP-98A; Softron, Tokyo, Japan) in a conscious situation at day 28. The results were averaged.

Morphological Analysis

The excised aortic tree was photographed, after which the external aortic diameters were measured at the aortic arch, thoracic aorta, suprarenal aorta, and abdominal aorta using ImageJ (National Institutes of Health, Bethesda, MD). An aneurysm was defined based on a $\geq 50\%$ increase in the external aorta width compared with controls (WT mice, 0.76 mm; OPG^{-/-} mice, 0.73 mm in diameter, mean value obtained from 11 and 6 sham mice, respectively).

Histology and Immunohistochemistry

The cross-sections (4 μm) of the aortic arch, descending thoracic aorta, suprarenal aorta, and abdominal aorta were stained with hematoxylin–eosin, Sirius red (for collagen), Victoria blue (for elastin), and alcian blue (for proteoglycan). The semi-quantitative deposition of collagen, elastin, and proteoglycan was evaluated by using WinROOF 2018 (Mitani Co., Tokyo, Japan). Images covering the entire field of the aortic sections were captured under the same lighting conditions at $\times 100$ magnification (one image) for medial and adventitial thickness and $\times 200$ magnification (4–6 images) for elastin, collagen, and alcian blue. All images were analyzed under the same threshold and averaged. The medial and adventitial thicknesses were calculated as mean values for the 4 measurements taken orthogonal to each other in the cross-sections. The numbers of elastic lamina breaks (focal dissection) in the elastic layers were counted from the luminal to abluminal side^{22–24} and then summed. Histological evaluation was performed by 3 observers in a blind manner (T. T., Aya Kawano, Yukiko Kawagoe). To detect the immunoreactivity for osteoprotegerin, deparaffinized tissue sections were autoclaved at 121°C for 20 minutes in 10 mmol/L citrate buffer (pH 6.0). The staining protocol followed the manufacturer's instructions (Anti-Goat HRP-DAB Cell & Tissue Staining Kit, catalog number CTS008, R&D Systems). In brief, tissue sections were

immersed in 3% hydrogen peroxide for 5 minutes and incubated with serum blocking reagent for 15 minutes. Then, the sections were incubated with avidin for 15 minutes and then with biotin blocking reagents for 15 minutes. Tissue sections were incubated with the polyclonal primary antibody against mouse osteoprotegerin (5 $\mu\text{g}/\text{mL}$, catalog number AF459, R&D Systems) in Can Get Signal immunostaining solution A (TOYOBO, Osaka, Japan) at 4°C overnight.²⁵ The slides were incubated with biotinylated secondary antibody for 30 minutes, followed by incubation with high sensitivity streptavidin conjugated to horseradish peroxidase for 30 minutes. The immunoreactivity was visualized with 0.05% 3, 3'-diaminobenzidine containing hydrogen peroxide and counterstained with hematoxylin. The slide sections were dehydrated in xylene and coverslipped. We scanned the slides at $\times 40$ magnification using an Olympus BX53F microscope (Olympus, Tokyo, Japan). Negative control staining was performed by omitting the first antibody (data not shown).

Micro-Computed Tomography

After sacrificing the mouse, the right-lower extremity was taken and examined by micro-computed tomography scan (ScanXmate-L090H; Comscantecno, Kanagawa, Japan), as previously described.^{26,27} The trabecular bone microstructure of the tibiae was analyzed by using a 3-dimensional image analysis system (TRI/3D-BON; Ratoc System Engineering Co. Ltd., Tokyo, Japan). We examined the secondary trabecular area at the proximal tibia metaphysis (2.0-mm trimming) and determined the bone volume/tissue volume (%).

RANKL Concentration

The RANKL concentration was measured in mouse plasma using Quantikine ELISA kit (R & D Systems, Minneapolis, MN, USA).

RT² Profiler PCR Array Assay and Volcano Plot Analysis

The whole aortic tree was pulverized in Isogen (Nippon Gen), and total RNA was extracted using RNeasy Mini Kit (QIAGEN, Hilden, Germany). Thereafter, 1 μg of total RNA was used to synthesize complementary DNA using RT² First Strand Kit (QIAGEN), and Extracellular Matrix and Adhesion Molecules RT² profiler PCR array (QIAGEN) was performed in a 96-well plate using a Real-Time PCR System (ABI Prism 7300 Sequence Detector, Applied Biosystems) according to the manufacturer's protocol. Data were presented as $2^{-\Delta C_T}$ ($\Delta C_T = C_T$ in each gene of interest – average C_T in reference gene) in an Excel-based PCR Array data template

provided by QIAGEN and C_T in the reference gene was determined by averaging β -actin, β_2 -microglobulin, GAPDH, and glucuronidase β . The distribution of gene expression fold changes by plotting the logarithm and P values by plotting the negative logarithm were analyzed by Free web-based RT² Profiler PCR Array Data Analysis software and presented as volcano plots.

Real-Time Quantitative PCR

A total of 3 μ g of total RNA was used as a template for synthesizing complementary DNA with Invitrogen SuperScript II reverse transcriptase. Thereafter, complementary DNA was amplified using oligonucleotide primers and probes labeled with 6-carboxy-fluorescein as reporter fluorescence and with 6-carboxy-tetramethyl-rhodamine as quencher fluorescence via real-time quantitative PCR. The oligonucleotide sequences of probes and primers for mouse periostin were purchased from Thermo Fisher Scientific (TaqMan Gene Expression Assays; Mm01284919_m1). The gene expression levels were normalized relative to the level of 18S ribosomal RNA.²⁸

Statistical Analysis

Data were analyzed in GraphPad Prism 8 (La Jolla, CA, USA). Two variables were compared by performing Student t -test (effects of PEGylated hrOPG treatment), and multiple variables were compared by performing 2-way analysis of variance (genotype \times Ang II), followed by the Bonferroni post-hoc test. Survival rate was analyzed by log-rank test. The incidence of aortic rupture and dissection were analyzed using Chi-square test in Excel 2010 software. Size of samples and detailed statistical tests were described in figure legends. We presented the data as means \pm SEM, and $P < 0.05$ was considered significant.

RESULTS

OPG^{-/-} Mice Administered Ang II Displays High Mortality Attributable to Aortic Rupture

OPG^{-/-} mice showed severe osteoporosis up to adolescence.^{20,29} Subcutaneous Ang II administration to these mice fed with normal chow promoted higher mortality relative to that of other groups over the 28-day experimental period ($P < 0.0001$ by log-rank test, Figure 1A). The causes of death were pleural hemorrhage, peritoneal hemorrhage, heart failure, and undetermined in 4, 6, 1, and 4 mice, respectively. Representative images of fatal ruptured aorta with hemorrhage outside the vessel wall are shown in Figure 1B. The incidences of fatal aortic rupture (Chi-square, 8.024, $P = 0.005$, Figure 1C) and aortic dissection (Chi-square, 4.285, $P = 0.038$, Figure 1D) were greater in OPG^{-/-} mice than

in WT mice administered with Ang II. Ang II infusion promoted significantly greater aortic diameter at the suprarenal aorta in WT and OPG^{-/-} mice than that in sham mice (Figure 1E), with no difference in the incidence of aneurysm formation (WT mice, 5/15; OPG^{-/-} mice, 7/11, Chi-square, 2.345, $P = 0.126$). Among the surviving mice, Ang II raised systolic blood pressure equivalently at day 28 in WT and OPG^{-/-} mice ($P = 0.512$ by unpaired t -test) (Figure 1F).

Histological Alterations in OPG^{-/-} and WT Mice Administered Ang II

Ang II infusion showed increased media thicknesses at the descending thoracic aorta and suprarenal aorta of WT and OPG^{-/-} mice, which was greater in former than in the latter OPG^{-/-} mice (Figure 2A through 2D). In addition, Ang II infusion promoted increased adventitia thicknesses at the suprarenal aorta in WT and OPG^{-/-} mice, which was greater in the former than in the latter (Figure 2E through 2H). Ang II infusion decreased the percentage of collagen (Figure 2I through 2L) occupying the media to a similar extent between the WT and OPG^{-/-} mice. Elastin occupying the media decreased in OPG^{-/-} regardless of Ang II infusion (Figure 3A through 3D). However, Ang II infusion promoted a greater number of elastin breaks at the suprarenal aorta in OPG^{-/-} mice than in WT mice (Figure 3E through 3H). Ang II infusion tended to increase the area for proteoglycan at the medial layer of aortic arch, thoracic aorta, and suprarenal aorta in WT and OPG^{-/-} mice (Figure 3I through 3L). Figure 4A through 4H shows a representative collagen (Figure 4A and 4E), elastin (Figure 4B and 4F), proteoglycan (Figure 4C and 4G), and osteoprotegerin (Figure 4D and 4H) in WT and OPG^{-/-} mice administered Ang II. The intense staining of osteoprotegerin was not limited to the inner side of aortic wall (Figure 4D) but throughout the medial layer (Figure S1A through S1H), and the distribution was consistent with that of proteoglycan (Figure 4C) in WT mice. Osteoprotegerin immunoreactivity shown by proteoglycan was absent in OPG^{-/-} mice (Figure 4G and 4H).

Increased Periostin Expression in Ang II-Infused OPG^{-/-} Mice

To elicit the candidate molecule to link the RANKL and osteoprotegerin, we used PCR array analysis, focusing on the extracellular matrix and adhesion molecule in the aortae of WT and OPG^{-/-} mice with and without Ang II administration. In the sham-treatment groups, the aortae of OPG^{-/-} mice were characterized by increasing thrombospondin 1 (2.59-folds, $P = 0.0002$), matrix metalloproteinase 8 (2.63-folds, $P = 0.045$), and osteopontin (2.9-folds, $P = 0.039$) levels and by decreasing collagen type III, $\alpha 1$ (-2.94-folds, $P = 0.026$) levels compared with WT mice (Figure 5A). In the

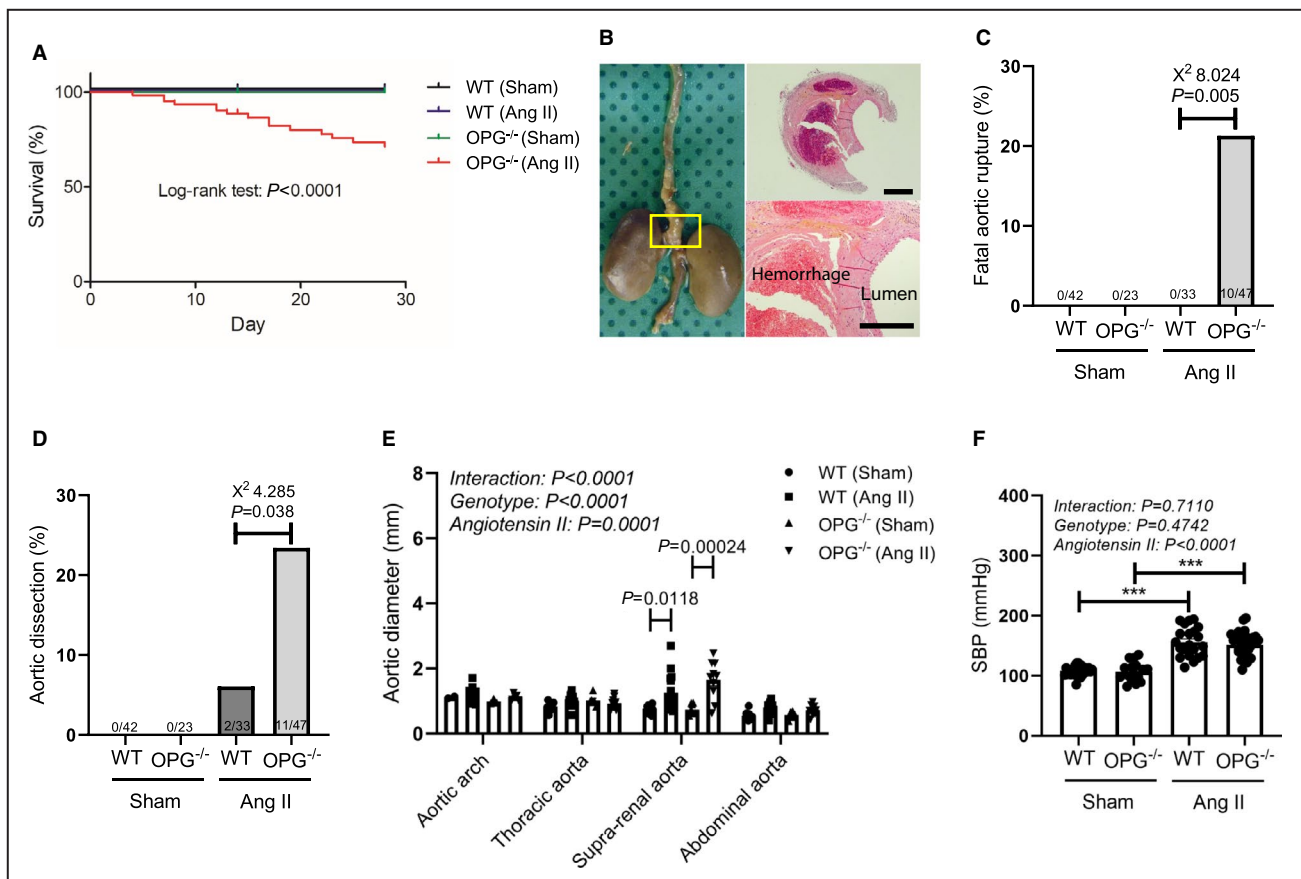


Figure 1. Survival, fatal aortic rupture, aortic dissection, aortic diameter, and systolic blood pressure in wild-type (WT) and OPG^{-/-} mice with and without angiotensin II (Ang II) administration for 28 days.

A, Survival rate. WT mice (Sham), n=42; WT mice (Ang II), n=33; OPG^{-/-} mice (Sham), n=23; OPG^{-/-} mice (Ang II), n=47. **B**, Example of an OPG^{-/-} mouse administered Ang II that died because of a fatal aortic rupture (**B**). The aorta shown in the square area was cut vertically and magnified under a microscope. Bar, 200 μ m. H indicates hemorrhage; and L, lumen. **C** and **D**, Incidence of fatal aortic rupture (**C**), and aortic dissection (**D**) in the surviving mice at day 28. Numbers in the panel indicate the animal numbers used (denominator) and those with aortic rupture or aortic dissection (numerator). The Chi-squared test gave a value of 8.024, $P=0.005$ for aortic rupture, and 4.285, $P=0.038$ for aneurysm formation in the WT and OPG^{-/-} mice stimulated by Ang II. **E**, Aortic diameter at the aortic arch, (descending) thoracic aorta, suprarenal aorta, and abdominal aorta at 28 days with and without Ang II administration in WT and OPG^{-/-} mice. **F**, Systolic blood pressure at 28 days with and without Ang II administration in WT and OPG^{-/-} mice (Sham: WT, n=28, OPG^{-/-}, n=16; Ang II: WT, n=21, OPG^{-/-}, n=30). Data are presented as a dot plot with means \pm SEM and analyzed by 2-way analysis of variance, followed by the Bonferroni post-hoc test. Ang II indicates angiotensin II; OPG^{-/-}, osteoprotegerin gene-knockout; and WT, wild-type. *** $P<0.001$.

28-day-Ang II treatment group, periostin expression was 2.5-fold higher ($P=0.007$) in OPG^{-/-} mice than in WT mice (Figure 5B). Real-time quantitative PCR confirmed that the magnitude of increase in periostin expression was higher in OPG^{-/-} mice than in WT mice (Figure 5C). All the genes identified by this analysis are listed in Table S1.

Recombinant Osteoprotegerin Administration Reversed All-Cause Mortality, Aortic Rupture, and Aortic Dissection in OPG^{-/-} Mice

PEGylated hrOPG administered to Ang II-stimulated OPG^{-/-} mice (n=39) promoted a decrease in all-cause

mortality (-22%), aortic rupture (-13%), and aortic dissection (-23%) relative to those in mice not receiving the same treatment (Figure 6A). The administration did not affect systolic blood pressure (Figure 6B, $P=0.0931$). The treatment increased bone volume/tissue volume at the tibia metaphysis (Figure 6C, $P<0.0001$) and decreased the concentration of soluble RANKL (Figure 6D, $P=0.0012$) and the periostin expression (Figure 6E, $P=0.0011$). During morphological analysis, the administration decreased the aortic diameter at the suprarenal aorta (Figure 6F, $P<0.0001$), the thickness of the adventitia at the aortic arch (Figure 6H, $P=0.0296$) and suprarenal aorta (Figure 6H, $P=0.0274$), and the numbers of elastin breaks (Figure 6J, $P=0.0539$) at the suprarenal aorta. However, the administration did not

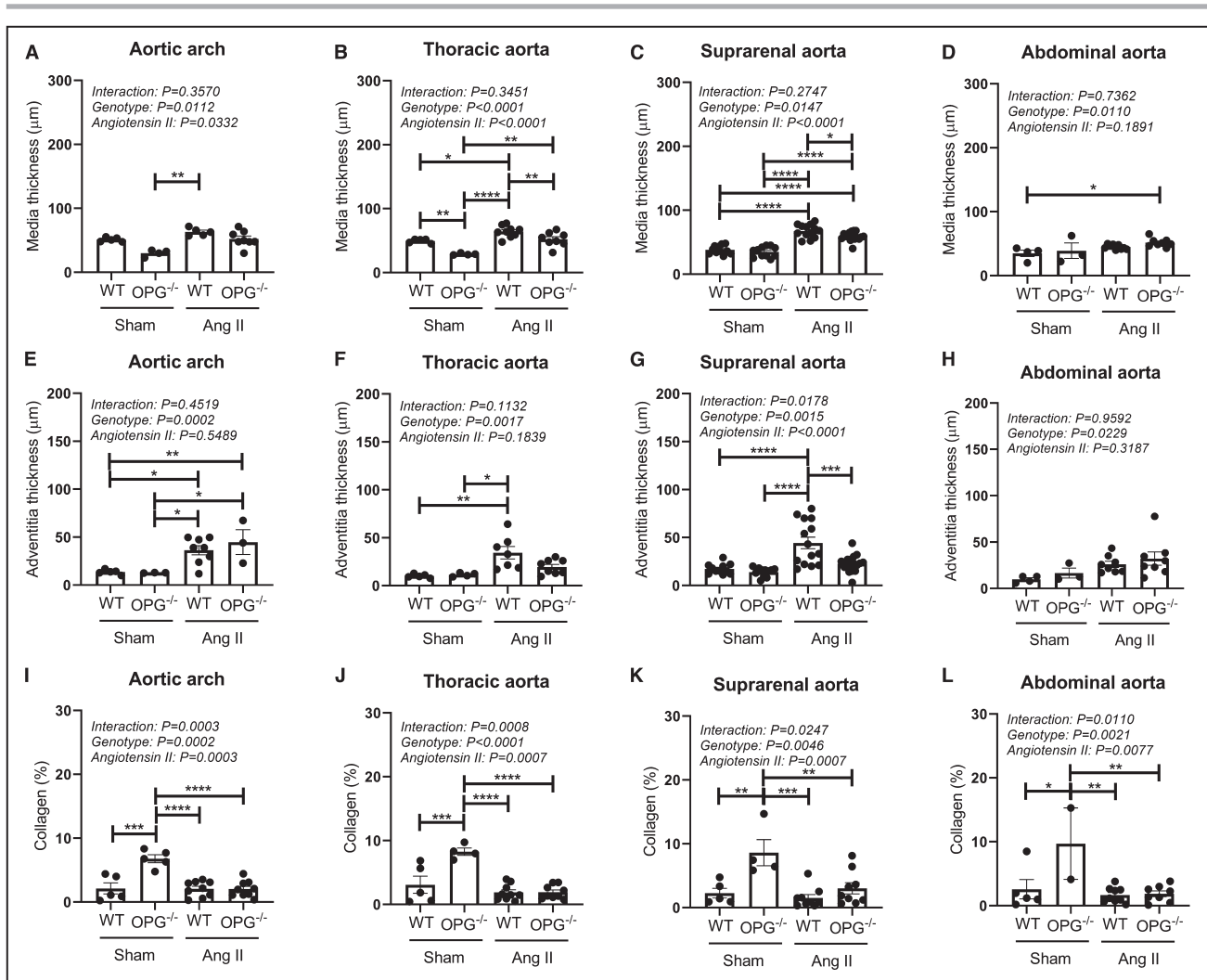


Figure 2. Histological characteristics of wild-type (WT) and osteoprotegerin gene-knockout (OPG^{-/-}) mice with and without angiotensin II (Ang II) infusion at 28 days.

A through D, Media thickness (aortic arch, Sham: WT, n=5, OPG^{-/-}, n=4; Ang II: WT, n=5, OPG^{-/-}, n=8; thoracic aorta, Sham: WT, n=5, OPG^{-/-}, n=4; Ang II: WT, n=9, OPG^{-/-}, n=8; suprarenal aorta, Sham: WT, n=11, OPG^{-/-}, n=11; Ang II: WT, n=13, OPG^{-/-}, n=16; abdominal aorta, Sham: WT, n=4, OPG^{-/-}, n=3; Ang II: WT, n=9, OPG^{-/-}, n=8); **(E through H)** adventitia thickness (aortic arch, Sham: WT, n=5, OPG^{-/-}, n=3; Ang II: WT, n=8, OPG^{-/-}, n=3; thoracic aorta, Sham: WT, n=5, OPG^{-/-}, n=4; Ang II: WT, n=7, OPG^{-/-}, n=8; suprarenal aorta, Sham: WT, n=11, OPG^{-/-}, n=11; Ang II: WT, n=14, OPG^{-/-}, n=17; abdominal aorta, Sham: WT, n=4, OPG^{-/-}, n=3; Ang II: WT, n=8, OPG^{-/-}, n=8); **(I through L)** percent collagen (aortic arch, Sham: WT, n=5, OPG^{-/-}, n=5; Ang II: WT, n=9, OPG^{-/-}, n=9; thoracic aorta, Sham: WT, n=5, OPG^{-/-}, n=5; Ang II: WT, n=9, OPG^{-/-}, n=9; suprarenal aorta, Sham: WT, n=5, OPG^{-/-}, n=4; Ang II: WT, n=9, OPG^{-/-}, n=9; abdominal aorta, Sham: WT, n=5, OPG^{-/-}, n=2; Ang II: WT, n=9, OPG^{-/-}, n=8). Data are presented as a dot plot with means±SEM and analyzed via 2-way analysis of variance, followed by the Bonferroni post-hoc test. Ang II indicates angiotensin II; OPG^{-/-}, osteoprotegerin gene-knockout; and WT, wild-type. **P*<0.05, ***P*<0.01, ****P*<0.001, *****P*<0.001.

affect the media thickness (Figure 6G) or elastin occupying the media (Figure 6I).

DISCUSSION

Our data suggested that osteoprotegerin plays an important role in maintaining the structural integrity of the aorta in mice with Ang II-induced hypertension. The incidences of aortic rupture and dissection were greater in OPG^{-/-} mice than in WT mice. However, recombinant

osteoprotegerin supplementation in OPG^{-/-} mice reversed the increase in morbidity, supporting the evidence that osteoprotegerin functions to protect the aortic structure. Ex-vivo analysis demonstrated that the suprarenal aorta selectively increased the diameter mostly because of the dissection of the aneurysm in WT and OPG^{-/-} mice. However, a hematoma was found in the chest cavity at equivalent prevalence to peritoneal hemorrhage in OPG^{-/-} mice. The initiation of the medial tear and the subsequent adventitial dissection occurred near the intercostal orifice of the thoracic

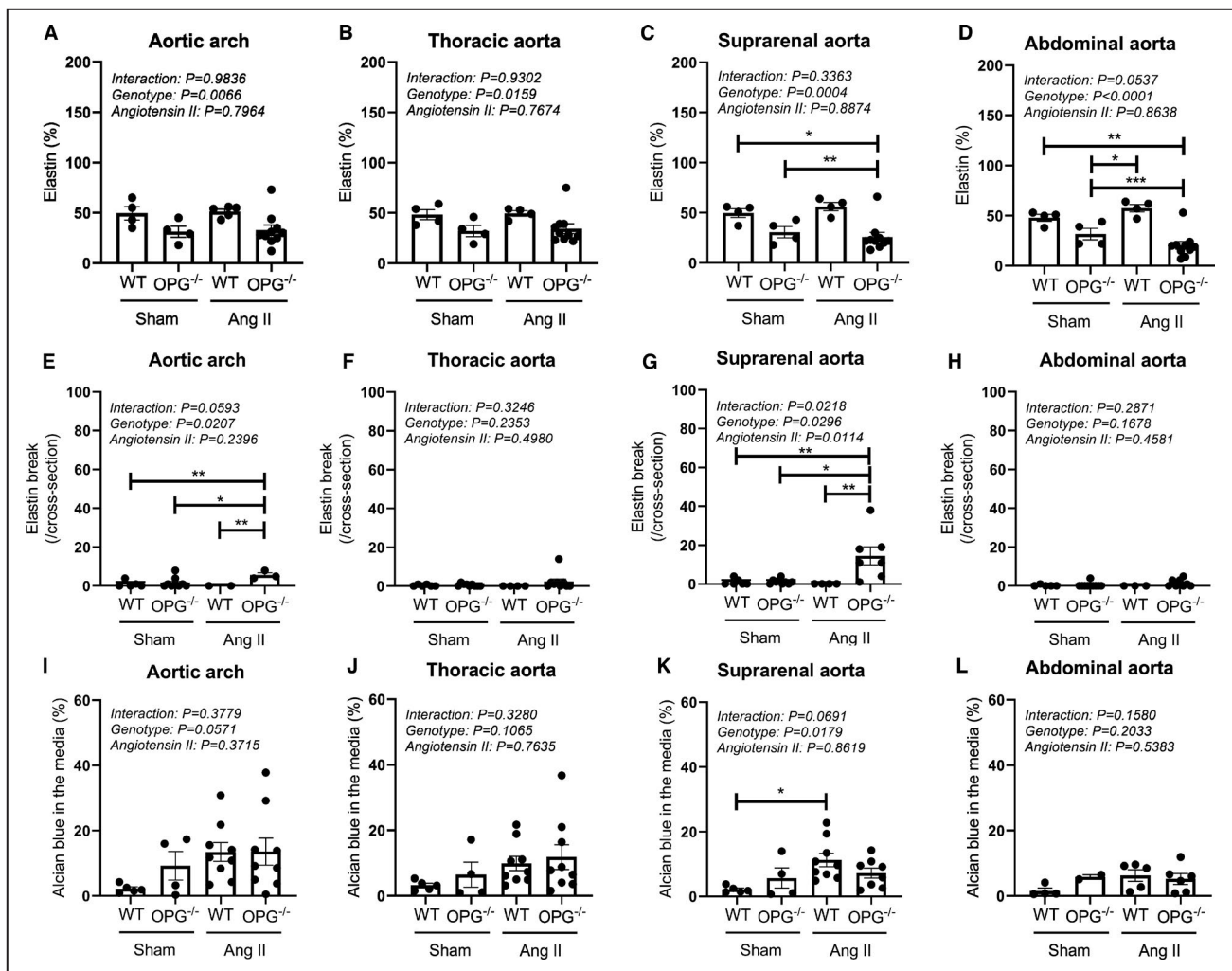


Figure 3. Histological characteristics of wild-type (WT) and osteoprotegerin gene-knockout (OPG^{-/-}) mice with and without angiotensin II (Ang II) infusion at 28 days.

A through D, Percent elastin (aortic arch, Sham: WT, n=4, OPG^{-/-}, n=5; Ang II: WT, n=4, OPG^{-/-}, n=10; thoracic aorta, Sham: WT, n=4, OPG^{-/-}, n=4; Ang II: WT, n=4, OPG^{-/-}, n=10; suprarenal aorta, Sham: WT, n=4, OPG^{-/-}, n=4; Ang II: WT, n=4, OPG^{-/-}, n=10; abdominal aorta, Sham: WT, n=4, OPG^{-/-}, n=4; Ang II: WT, n=4, OPG^{-/-}, n=10); **(E through H)** elastin breaks (aortic arch, Sham: WT, n=5, OPG^{-/-}, n=2; Ang II: WT, n=9, OPG^{-/-}, n=3; thoracic aorta, Sham: WT, n=6, OPG^{-/-}, n=4; Ang II: WT, n=9, OPG^{-/-}, n=9; suprarenal aorta, Sham: WT, n=4, OPG^{-/-}, n=4; Ang II: WT, n=9, OPG^{-/-}, n=7; abdominal aorta, Sham: WT, n=5, OPG^{-/-}, n=3; Ang II: WT, n=10, OPG^{-/-}, n=8); **(I through L)** alcian blue (aortic arch, Sham: WT, n=5, OPG^{-/-}, n=4; Ang II: WT, n=9, OPG^{-/-}, n=9; thoracic aorta, Sham: WT, n=5, OPG^{-/-}, n=4; Ang II: WT, n=9, OPG^{-/-}, n=9; suprarenal aorta, Sham: WT, n=5, OPG^{-/-}, n=4; Ang II: WT, n=9, OPG^{-/-}, n=9; abdominal aorta, Sham: WT, n=4, OPG^{-/-}, n=2; Ang II: WT, n=6, OPG^{-/-}, n=6). Data are presented as a dot plot with means±SEM and analyzed via 2-way analysis of variance, followed by the Bonferroni post hoc test. **P*<0.05, ***P*<0.01, ****P*<0.001. Ang II indicates angiotensin II; OPG^{-/-}, osteoprotegerin gene-knockout; and WT, wild-type.

aorta.³⁰ Micro-computed tomography scan used for bone morphometrical analysis in this study did not reach the visualizing fine vascular structure. Moreover, we could not determine the exact dissecting and rupture sites, and our ex-vivo histological feature was not validated via micro-computed tomography imaging.

Degradation of elastin in the aorta is associated with increase in the wall thickness and stiffness with aging.³¹ The passive mechanical force and other chemical alterations enhanced the fragility of elastin,³¹

and alteration in the smooth muscle cell phenotype³² contributed to the pathogenesis of aortic rupture and dissection. In this experiment, Ang II-infused OPG^{-/-} mice showed exaggerated elastin fragmentation at the suprarenal aorta regardless of using thinner media when compared with WT mice, suggesting that inappropriate pulsatile wall strain may cause elastin fragmentation mechanically.³¹ Moreover, the effects of osteoprotegerin deficiency on factors weakening the aortic wall may involve the following points. We

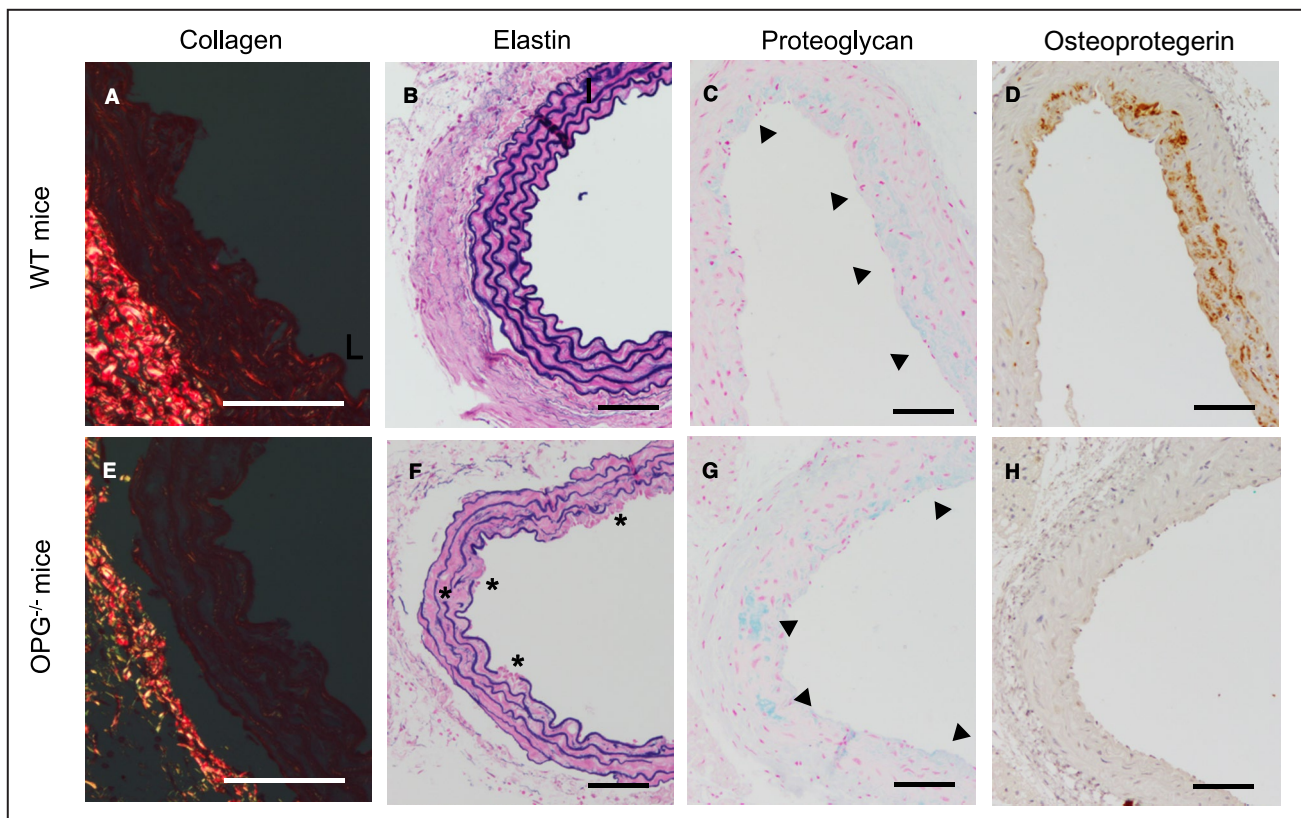


Figure 4. Representative images of collagen (A and E), elastin (B and F), proteoglycan (C and G), and osteoprotegerin (D and H) are shown.

The asterisks in (F) indicate the part of elastin break (focal dissection). Triangles in (C and G) indicate the distribution of proteoglycan assessed by alcian blue; bar 50 μm . OPG^{-/-} indicates osteoprotegerin gene-knockout; and WT, wild-type.

previously reported that the soluble RANKL concentration was elevated in OPG^{-/-} mice.²⁶ The present study showed that recombinant osteoprotegerin administration to these mice decreased the RANKL concentration. RANKL stimulates the activity of elastin degrading enzyme, matrix metalloproteinase-9,^{33,34} which might explain the increase in elastin breaks in OPG^{-/-} mice. In support of our findings, Tanaka et al³³ reported that neutralization with the RANKL antibody inhibited the dissecting aneurysm in Ang II-infused apolipoprotein E-deficient mice. In this study, Ang II-infused OPG^{-/-} mice significantly increased periostin mRNA expression, with values greater than that observed in the other groups. By contrast, hrOPG supplementation decreased periostin mRNA expression. Bonet et al³⁵ reported a novel mechanism of RANKL to increase the bone fragility in a periostin-dependent fashion. Periostin is a matricellular protein that regulates extracellular matrix formation and is upregulated in human abdominal aortic aneurysm.³⁶ Our data suggested that RANKL links to periostin alters the vascular structure when osteoprotegerin is deficient. Adventitial layer consists predominantly of type I and III collagens and contributes in the prevention of aortic rupture at high blood pressures, which is accompanied by changing

the type I and III ratio.³⁷⁻³⁹ The newly synthesized type III collagen, which is susceptible to proteolysis, is increased in human abdominal aortic aneurysm.⁴⁰ OPG^{-/-} mice shows the discordant expression of type III collagen in homogenates of whole aorta with its histological distribution at the adventitia, suggesting the distinct synthesis and metabolism in 3 layers of the aortic wall. The Ang II-infused OPG^{-/-} mice demonstrated a trend of higher collagen type III than WT mice, however, it did not reach at significant difference of collagen type I and III ratio (Figure S2). Meanwhile, this study shows that the adventitial layer was thinner at the suprarenal aorta in the Ang II-infused OPG^{-/-} mice than in the WT mice. Thus, structural alternation at the adventitial layer may be another cause of aortic rupture induction in Ang II-infused OPG^{-/-} mice.

Osteoprotegerin was positively stained in areas where proteoglycan is distributed in the aortic wall of Ang II-infused WT mice. Osteoprotegerin binds to proteoglycan via its heparin-binding domain (domain 7)⁴¹⁻⁴⁵ and activates focal adhesion kinase and extracellular signal-regulated kinase,⁴⁵⁻⁴⁸ which are crucial for vascular smooth muscle cell survival.^{32,49} Moreover, recombinant osteoprotegerin stimulates the proliferation and extracellular matrix synthesis independent of

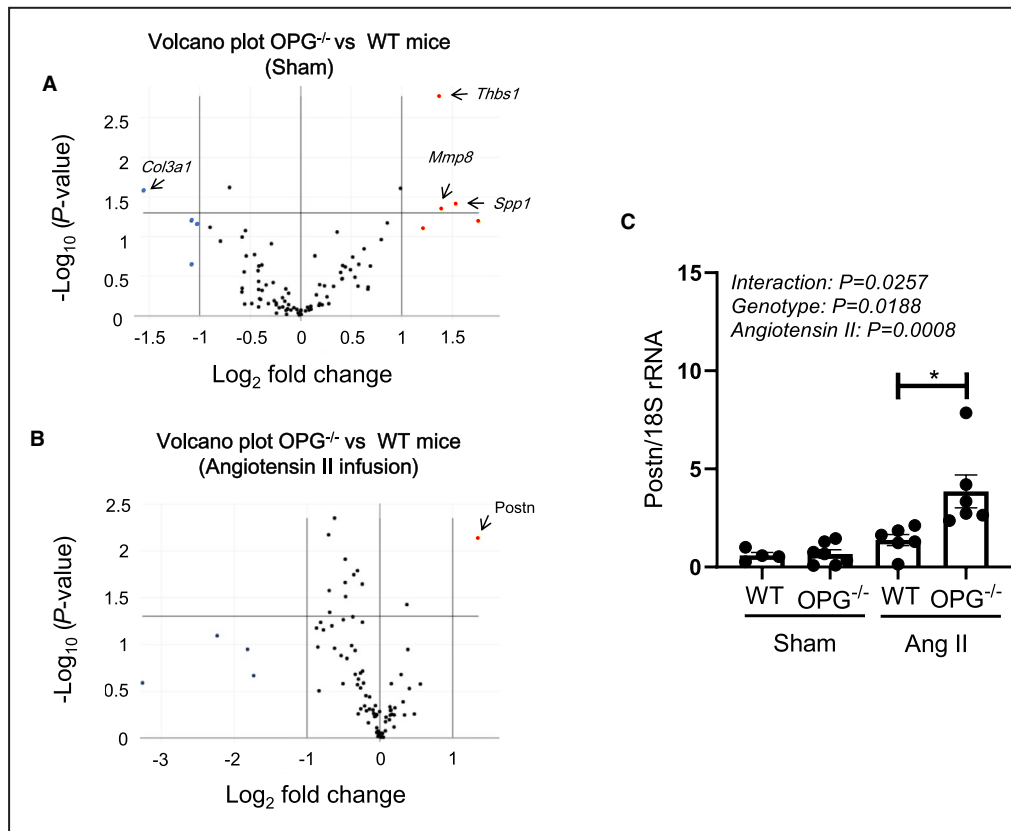


Figure 5. Volcano plots graphs of mouse aorta assessed by polymerase chain reaction array.

Gene expressions between osteoprotegerin gene-knockout (OPG^{-/-}) and wild-type (WT) mice groups without (A) and with (B) angiotensin II infusion (Sham: WT, n=4, OPG^{-/-}, n=4; Ang II: WT, n=4, OPG^{-/-}, n=6). Fold-regulation threshold >2, and $P<0.05$ from the Student *t*-test. Each gene >2 was highlighted in red, whereas <2 was highlighted in blue. *Thbs1*, thrombospondin 1; *Mmp8*, matrix metalloproteinase 8; *Spp1*, osteopontin; *Col3a1*, collagen type III, $\alpha 1$; *Postn*, periostin expression. The expression was normalized by averaging the Ct in the reference gene (β -actin, β_2 -microglobulin, and GAPDH). C, Real-time quantitative PCR analysis for periostin in WT mice and OPG^{-/-} mice without and with Ang II infusion for 28 days (Sham: WT, n=4, OPG^{-/-}, n=7; Ang II: WT, n=6, OPG^{-/-}, n=6). Data are presented as dot plot with means \pm SEM and analyzed via 2-way analysis of variance, followed by the Bonferroni post-hoc test. Ang II indicates angiotensin II; OPG^{-/-}, osteoprotegerin gene-knockout; and WT, wild-type. * $P<0.05$.

RANKL activity in vascular smooth muscle cells.^{46,50–52} It remains inconclusive whether osteoprotegerin plays a protective role in rodent models of abdominal aortic aneurysm.^{53–56} Vorkapic et al⁵⁵ reported that human recombinant full-length osteoprotegerin (0.24–0.36 mg/kg, subcutaneous administration with implanted mini-pump for 28 days) did not affect the development of abdominal aortic aneurysm in Ang II-infused apolipoprotein E-deficient mice. To address whether this was a matter of the concentration of recombinant osteoprotegerin interacting with the heparin-binding domain and/or it depended on rodent models to develop atherosclerosis, we used the modification of hrOPG with PEGylation at the C-terminus region (heparin-binding domain), which failed to interact with heparin sulfate proteoglycan.²¹ Thus, our results suggested that hrOPG prevented the rupture of mice aorta by blocking the bioactivity

of RANKL in Ang II-infused non-atherosclerosis mice. We used the experimental OPG^{-/-} data from the first half of the study as reference for hrOPG administration. Accordingly, we confirmed the efficacy of hrOPG by decreasing the circulating RANKL concentration and increasing the bone density; however, we acknowledged that the inadequate vehicle control greatly reduced the robustness and reproducibility of our evidence. Only a few studies have investigated the association between osteoprotegerin and aortic dissection in humans; therefore, further studies are needed to clarify the role of osteoprotegerin as a biomarker and therapeutic target for aortic rupture and dissection.

In summary, the study findings indicated that osteoprotegerin might protect against aortic rupture and dissection in Ang II-induced hypertension by inhibiting RANKL activity and periostin expression.

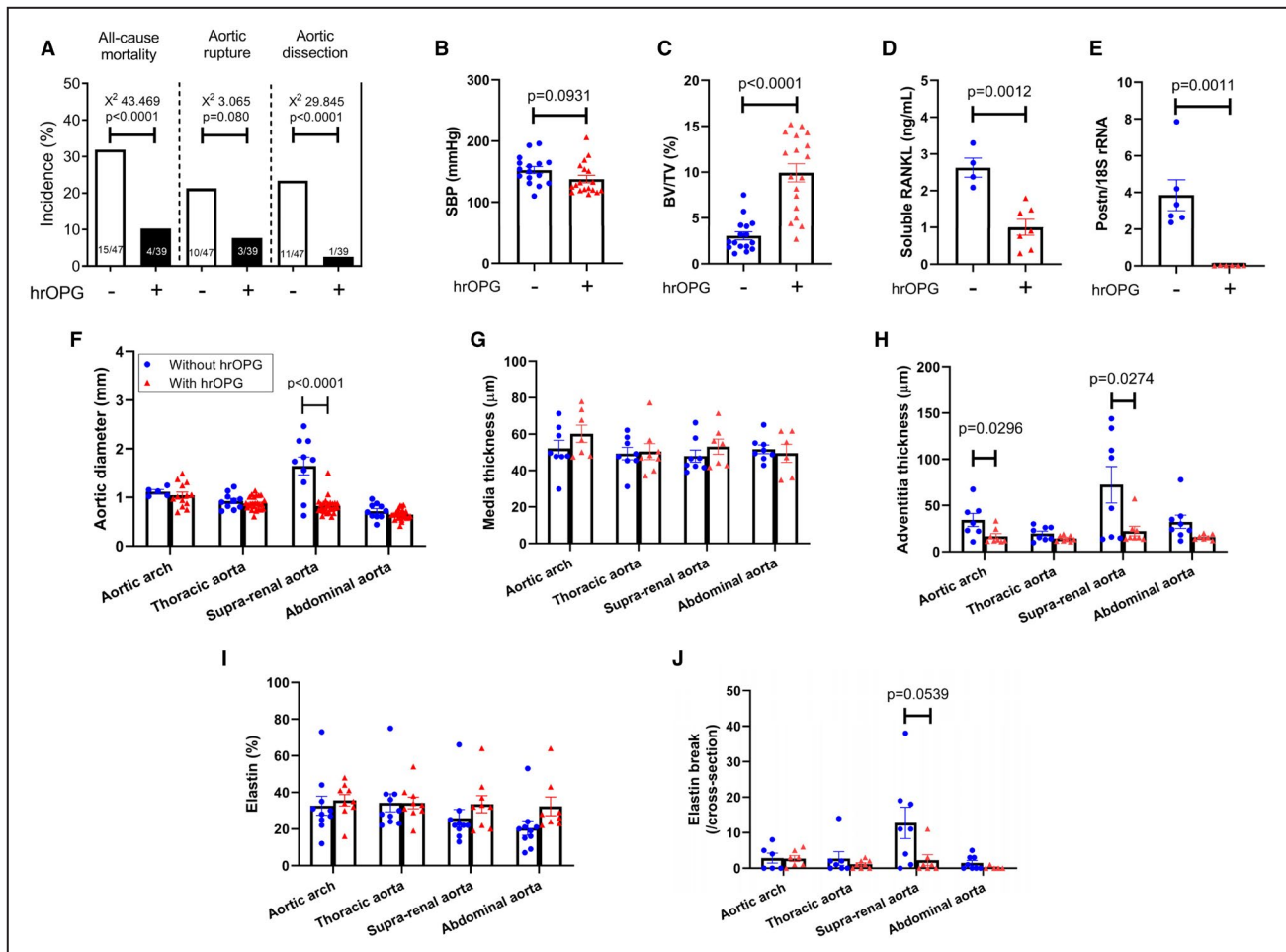


Figure 6. (A) Effects of poly(PEG)-human recombinant osteoprotegerin (hrOPG) treatment on the incidence of all-cause mortality, aortic rupture, and aortic dissection; (B) systolic blood pressure; (C) bone volume/tissue volume at the tibial metaphysis; (D) soluble receptor activator of nuclear factor- κ B ligand concentration; and (E) periostin expression; (F) aortic diameter; (G through J) histological analyses (G, media thickness; H, adventitia thickness; I, percent elastin; J, numbers of elastin breaks) in angiotensin II-infused osteoprotegerin gene-knockout mice.

Ten mg/kg of PEGylated human recombinant osteoprotegerin (hrOPG) was administered intraperitoneally to the Ang II-infused osteoprotegerin gene-knockout mice every 2 days from day 1 to 28. **A**, Numbers in the panel indicate the animal numbers used (denominator) and the incidences of all-cause mortality, aortic rupture, or aortic dissection (numerator). The Chi-square test was used for statistical analysis. **B** through **J**, Data are presented as a dot plot with means \pm SEM without and with PEGylated hrOPG treatment. Data are analyzed by Student *t*-test. BV/TV indicates bone volume/tissue volume; SBP, systolic blood pressure; Postn, periostin expression; and RANKL, receptor activator of nuclear factor- κ B ligand.

ARTICLE INFORMATION

Received January 10, 2022; accepted March 16, 2022.

Affiliations

Division of Internal Medicine, Cardiovascular Medicine and Nephrology, Faculty of Medicine (T.T., M.O.), Department of Pathology, Faculty of Medicine (A.Y., Y.A.), Division of Orthopedic Surgery, Department of Medicine of Sensory and Motor Organs, Faculty of Medicine (T.F., E.C.), and Frontier Science Research Center (J.K., K.K.), University of Miyazaki, Miyazaki, Japan; Institute for Oral Science (M.K., Y.N.) and Department of Biochemistry (N.U.), Matsumoto Dental University, Nagano, Japan; Department of Diagnostic Pathology, Nara Medical University, Nara, Japan (Y.S.); and Department of Pathology, National Cerebral and Cardiovascular Center, Osaka, Japan (K.H.).

Acknowledgments

We greatly thank to Ritsuko Sotomura, Nahoko Udatsu, Aya Kawano, Yukiko Kawagoe, and Shingo Takeda for their technical assistance.

Sources of Funding

This study was supported by grants-in-aid for Scientific Research (26461076, 19K08521 to Tsuruda) from the Japan Society for the Promotion of Science, and Clinical Research from Miyazaki University Hospital.

Disclosures

None.

Supplemental Material

Table S1
Figures S1–S2

REFERENCES

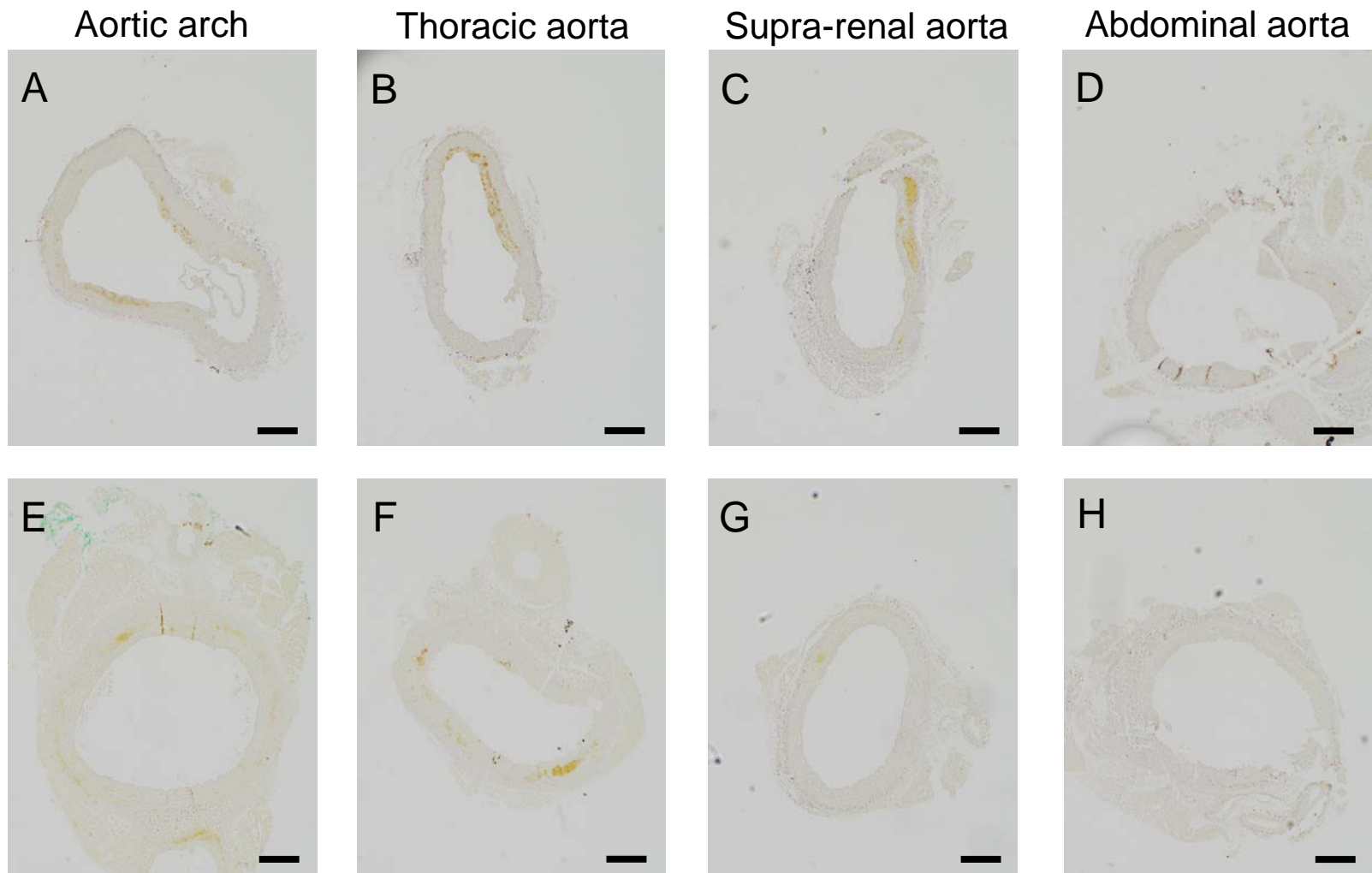
- Clouse WD, Hallett JW, Schaff HV, Spittell PC, Rowland CM, Ilstrup DM, Melton LJ. Acute aortic dissection: population-based incidence compared with degenerative aortic aneurysm rupture. *Mayo Clin Proc*. 2004;79:176–180. doi: 10.4066/79.2.176

2. Landenhed M, Engström G, Gottsäter A, Caulfield MP, Hedblad B, Newton-Cheh C, Melander O, Smith JG. Risk profiles for aortic dissection and ruptured or surgically treated aneurysms: a prospective cohort study. *J Am Heart Assoc*. 2015;4:e001513. doi: 10.1161/JAHA.114.001513
3. Evangelista A, Isselbacher EM, Bossone E, Gleason TG, Eusanio MD, Sechtem U, Ehrlich MP, Trimarchi S, Braverman AC, Myrmet T, et al. Insights from the international registry of acute aortic dissection: a 20-year experience of collaborative clinical research. *Circulation*. 2018;137:1846–1860. doi: 10.1161/CIRCULATIONAHA.117.031264
4. Nakashima Y. Pathogenesis of aortic dissection: elastic fiber abnormalities and aortic medial weakness. *Ann Vasc Dis*. 2010;3:28–36. doi: 10.3400/avd.AVDsaspv10002
5. Zhang X, Shen YH, LeMaire SA. Thoracic aortic dissection: are matrix metalloproteinases involved? *Vascular*. 2009;17:147–157. doi: 10.2310/6670.2008.00087
6. Humphrey JD. Possible mechanical roles of glycosaminoglycans in thoracic aortic dissection and associations with dysregulated transforming growth factor- β . *J Vasc Res*. 2013;50:1–10. doi: 10.1159/000342436
7. Wight TN, Merrilees MJ. Proteoglycans in atherosclerosis and restenosis: key roles for versican. *Circ Res*. 2004;94:1158–1167. doi: 10.1161/01.RES.0000126921.29919.51
8. Wu YJ, La Pierre DP, Wu J, Yee AJ, Yang BB. The interaction of versican with its binding partners. *Cell Res*. 2005;15:483–494. doi: 10.1038/sj.cr.7290318
9. Muñoz EM, Linhardt RJ. Heparin-binding domains in vascular biology. *Arterioscler Thromb Vasc Biol*. 2004;24:1549–1557. doi: 10.1161/01.ATV.0000137189.22999.3f
10. Lacey DL, Timms E, Tan H-L, Kelley MJ, Dunstan CR, Burgess T, Elliott R, Colombero A, Elliott G, Scully S, et al. Osteoprotegerin ligand is a cytokine that regulates osteoclast differentiation and activation. *Cell*. 1998;93:165–176. doi: 10.1016/S0092-8674(00)81569-X
11. Simonet WS, Lacey DL, Dunstan CR, Kelley M, Chang M-S, Lüthy R, Nguyen HQ, Wooden S, Bennett L, Boone T, et al. Osteoprotegerin: a novel secreted protein involved in the regulation of bone density. *Cell*. 1997;89:309–319. doi: 10.1016/S0092-8674(00)80209-3
12. Tsuda E, Goto M, Mochizuki S, Yano K, Kobayashi F, Morinaga T, Higashio K. Isolation of a novel cytokine from human fibroblasts that specifically inhibits osteoclastogenesis. *Biochem Biophys Res Commun*. 1997;234:137–142. doi: 10.1006/bbrc.1997.6603
13. Yasuda H, Shima N, Nakagawa N, Mochizuki S, Yano K, Fujise N, Sato Y, Goto M, Yamaguchi K, Kuriyama M, et al. Identity of osteoclastogenesis inhibitory factor (OCIF) and osteoprotegerin (OPG): a mechanism by which OPG/OCIF inhibits osteoclastogenesis in vitro. *Endocrinology*. 1998;139:1329–1337. doi: 10.1210/endo.139.3.5837
14. Osako MK, Nakagami H, Shimamura M, Koriyama H, Nakagami F, Shimizu H, Miyake T, Yoshizumi M, Rakugi H, Morishita R. Cross-talk of receptor activator of nuclear factor- κ B ligand signaling with renin-angiotensin system in vascular calcification. *Arterioscler Thromb Vasc Biol*. 2013;33:1287–1296. doi: 10.1161/ATVBAHA.112.301099
15. McGonigle JS, Giachelli CM, Scatena M. Osteoprotegerin and RANKL differentially regulate angiogenesis and endothelial cell function. *Angiogenesis*. 2009;12:35–46. doi: 10.1007/s10456-008-9127-z
16. Olesen P, Ledet T, Rasmussen LM. Arterial osteoprotegerin: increased amounts in diabetes and modifiable synthesis from vascular smooth muscle cells by insulin and TNF- α . *Diabetologia*. 2005;48:561–568. doi: 10.1007/s00125-004-1652-8
17. Whyte MP, Obrecht SE, Finnegan PM, Jones JL, Podgornik MN, McAlister WH, Mumm S. Osteoprotegerin deficiency and juvenile Paget's disease. *N Engl J Med*. 2002;347:175–184. doi: 10.1056/NEJMoa013096
18. Allen CA, Hart BL, Taylor CL, Clericuzio CL. Bilateral cavernous internal carotid aneurysms in a child with juvenile paget disease and osteoprotegerin deficiency. *AJNR Am J Neuroradiol*. 2008;29:7–8. doi: 10.3174/ajnr.A0755
19. Kerr NM, Cassinelli HR, DiMeglio LA, Tau C, Tüysüz B, Cundy T, Vincent AL. Ocular manifestations of juvenile Paget disease. *Arch Ophthalmol*. 2010;128:698–703. doi: 10.1001/archophthalmol.2010.76
20. Mizuno A, Amizuka N, Irie K, Murakami A, Fujise N, Kanno T, Sato Y, Nakagawa N, Yasuda H, Mochizuki S-I, et al. Severe osteoporosis in mice lacking osteoclastogenesis inhibitory factor/osteoprotegerin. *Biochem Biophys Res Commun*. 1998;247:610–615. doi: 10.1006/bbrc.1998.8697
21. Saito-Yabe M, Kasuya Y, Yoshigae Y, Yamamura N, Suzuki Y, Fukuda N, Honma M, Yano K, Mochizuki S-I, Okada F, et al. PEGylation of osteoprotegerin/osteoclastogenesis inhibitory factor (OPG/OCIF) results in decreased uptake into rats and human liver. *J Pharm Pharmacol*. 2010;62:985–994. doi: 10.1111/j.2042-7158.2010.01120.x
22. Luttun A, Lutgens E, Manderveld A, Maris K, Collen D, Carmeliet P, Moons L. Loss of matrix metalloproteinase-9 or matrix metalloproteinase-12 protects apolipoprotein E-deficient mice against atherosclerotic media destruction but differentially affects plaque growth. *Circulation*. 2004;109:1408–1414. doi: 10.1161/01.CIR.0000121728.14930.DE
23. Bai L, Beckers L, Wijnands E, Lutgens SPM, Herías MV, Saffig P, Daemen MJAP, Cleutjens K, Lutgens E, Biessen EAL, et al. Cathepsin K gene disruption does not affect murine aneurysm formation. *Atherosclerosis*. 2010;209:96–103. doi: 10.1016/j.atherosclerosis.2009.09.001
24. Trachet B, Piersigilli A, Fraga-Silva RA, Aslanidou L, Sordet-Dessimoz J, Astolfo A, Stampanoni MF, Segers P, Stergiopoulos N. Ascending aortic aneurysm in angiotensin II-infused mice: formation, progression, and the role of focal dissections. *Arterioscler Thromb Vasc Biol*. 2016;36:673–681. doi: 10.1161/ATVBAHA.116.307211
25. Koide M, Kobayashi Y, Ninomiya T, Nakamura M, Yasuda H, Arai Y, Okahashi N, Yoshinari N, Takahashi N, Udagawa N. Osteoprotegerin-deficient male mice as a model for severe alveolar bone loss: comparison with RANKL-overexpressing transgenic male mice. *Endocrinology*. 2013;154:773–782. doi: 10.1210/en.2012-1928
26. Tsuruda T, Sekita-Hatakeyama Y, Hao Y, Sakamoto S, Kurogi S, Nakamura M, Udagawa N, Funamoto T, Sekimoto T, Hatakeyama K, et al. Angiotensin II stimulation of cardiac hypertrophy and functional decompensation in osteoprotegerin-deficient mice. *Hypertension*. 2016;67:848–856. doi: 10.1161/HYPERTENSIONAHA.115.06689
27. Tsuruda T, Funamoto T, Udagawa N, Kurogi S, Nakamichi Y, Koide M, Chosa E, Asada Y, Kitamura K. Blockade of the angiotensin II type 1 receptor increases bone mineral density and left ventricular contractility in a mouse model of juvenile Paget disease. *Eur J Pharmacol*. 2019;859:172519. doi: 10.1016/j.ejphar.2019.172519
28. Hao Y, Tsuruda T, Sekita-Hatakeyama Y, Kurogi S, Kubo K, Sakamoto S, Nakamura M, Udagawa N, Sekimoto T, Hatakeyama K, et al. Cardiac hypertrophy is exacerbated in aged mice lacking the osteoprotegerin gene. *Cardiovasc Res*. 2016;110:62–72. doi: 10.1093/cvr/cvv025
29. Bucay N, Sarosi I, Dunstan CR, Morony S, Tarpley J, Capparelli C, Scully S, Tan HL, Xu W, Lacey DL, et al. Osteoprotegerin-deficient mice develop early onset osteoporosis and arterial calcification. *Genes Dev*. 1998;12:1260–1268. doi: 10.1101/gad.12.9.1260
30. Trachet B, Aslanidou L, Piersigilli A, Fraga-Silva RA, Sordet-Dessimoz J, Villanueva-Perez P, Stampanoni MFM, Stergiopoulos N, Segers P. Angiotensin II infusion into ApoE^{-/-} mice: a model for aortic dissection rather than abdominal aortic aneurysm? *Cardiovasc Res*. 2017;113:1230–1242. doi: 10.1093/cvr/cvx128
31. Duca L, Blaise S, Romier B, Laffargue M, Gayral S, El Btaoui H, Kaweck C, Guillot A, Martiny L, Debelle L, et al. Matrix ageing and vascular impacts: focus on elastin fragmentation. *Cardiovasc Res*. 2016;110:298–308. doi: 10.1093/cvr/cvv061
32. Michel JB, Jondeau G, Milewicz DM. From genetics to response to injury: vascular smooth muscle cells in aneurysms and dissections of the ascending aorta. *Cardiovasc Res*. 2018;114:578–589. doi: 10.1093/cvr/cvy006
33. Tanaka T, Kelly M, Takei Y, Yamanouchi D. RANKL-mediated osteoclastogenic differentiation of macrophages in the abdominal aorta of angiotensin II-infused apolipoprotein E knockout mice. *J Vasc Surg*. 2018;68:48S–59S.e41. doi: 10.1016/j.jvs.2017.11.091
34. Zhou L, Le Y, Tian J, Yang X, Jin R, Gai X, Sun Y. Cigarette smoke-induced RANKL expression enhances MMP-9 production by alveolar macrophages. *Int J Chron Obstruct Pulmon Dis*. 2019;14:81–91. doi: 10.2147/COPD.S190023
35. Bonnet N, Douni E, Perréard Lopreno G, Besse M, Biver E, Ferrari S. RANKL-induced increase in cathepsin K levels restricts cortical expansion in a periostin-dependent fashion: a potential new mechanism of bone fragility. *J Bone Miner Res*. 2021;36:1636–1645. doi: 10.1002/jbmr.4307
36. Yamashita O, Yoshimura K, Nagasawa A, Ueda K, Morikage N, Ikeda Y, Hamano K. Periostin links mechanical strain to inflammation in abdominal aortic aneurysm. *PLoS One*. 2013;8:e79753. doi: 10.1371/journal.pone.0079753
37. Lehoux S. Adventures in the adventitia. *Hypertension*. 2016;67:836–838. doi: 10.1161/HYPERTENSIONAHA.116.06375
38. Chow MJ, Turcotte R, Lin CP, Zhang Y. Arterial extracellular matrix: a mechanobiological study of the contributions and interactions of

- elastin and collagen. *Biophys J*. 2014;106:2684–2692. doi: 10.1016/j.bpj.2014.05.014
39. Wittig C, Szulcek R. Extracellular matrix protein ratios in the human heart and vessels: how to distinguish pathological from physiological changes? *Front Physiol*. 2021;12:708656. doi: 10.3389/fphys.2021.708656
 40. Bode MK, Soini Y, Melkko J, Satta J, Risteli L, Risteli J. Increased amount of type III pN-collagen in human abdominal aortic aneurysms: evidence for impaired type III collagen fibrillogenesis. *J Vasc Surg*. 2000;32:1201–1207. doi: 10.1067/mva.2000.109743
 41. Standal T, Seidel C, Hjertner Ø, Plesner T, Sanderson RD, Waage A, Borset M, Sundan A. Osteoprotegerin is bound, internalized, and degraded by multiple myeloma cells. *Blood*. 2002;100:3002–3007. doi: 10.1182/blood-2002-04-1190
 42. Lamoureux F, Picarda G, Garrigue-Antar L, Baud'huin M, Trichet V, Vidal A, Miot-Noirault E, Pitard B, Heymann D, Rédini F. Glycosaminoglycans as potential regulators of osteoprotegerin therapeutic activity in osteosarcoma. *Cancer Res*. 2009;69:526–536. doi: 10.1158/0008-5472.CAN-08-2648
 43. Mosheimer BA, Kaneider NC, Feistritz C, Djanani AM, Sturn DH, Patsch JR, Wiedermann CJ. Syndecan-1 is involved in osteoprotegerin-induced chemotaxis in human peripheral blood monocytes. *J Clin Endocrinol Metab*. 2005;90:2964–2971. doi: 10.1210/jc.2004-1895
 44. Li M, Yang S, Xu D. Heparan sulfate regulates the structure and function of osteoprotegerin in osteoclastogenesis. *J Biol Chem*. 2016;291:24160–24171. doi: 10.1074/jbc.M116.751974
 45. Baud'huin M, Duplomb L, Teletchea S, Lamoureux F, Ruiz-Velasco C, Maillason M, Redini F, Heymann MF, Heymann D. Osteoprotegerin: multiple partners for multiple functions. *Cytokine Growth Factor Rev*. 2013;24:401–409. doi: 10.1016/j.cytogfr.2013.06.001
 46. He Y, Zou PU, Lu Y, Jia D, Li X, Yang H, Tang L, Zhu Z, Tu T, Tai S, et al. Osteoprotegerin promotes intimal hyperplasia and contributes to intimal restenosis: role of an α V β 3/FAK dependent YAP pathway. *J Mol Cell Cardiol*. 2020;139:1–13. doi: 10.1016/j.yjmcc.2020.01.006
 47. Feng ZY, He ZN, Zhang B, Chen Z. Osteoprotegerin promotes the proliferation of chondrocytes and affects the expression of ADAMTS-5 and TIMP-4 through MEK/ERK signaling. *Mol Med Rep*. 2013;8:1669–1679. doi: 10.3892/mmr.2013.1717
 48. Kobayashi-Sakamoto M, Isogai E, Holen I. Osteoprotegerin induces cytoskeletal reorganization and activates FAK, Src, and ERK signaling in endothelial cells. *Eur J Haematol*. 2010;85:26–35. doi: 10.1111/j.1600-0609.2010.01446.x
 49. Bowen CJ, Calderón Giadrosic JF, Burger Z, Rykiel G, Davis EC, Helters MR, Benke K, Gallo MacFarlane E, Dietz HC. Targetable cellular signaling events mediate vascular pathology in vascular Ehlers-Danlos syndrome. *J Clin Invest*. 2020;130:686–698. doi: 10.1172/JCI130730
 50. Ovchinnikova O, Gylfe A, Bailey L, Nordström A, Rudling M, Jung C, Bergström S, Waldenström A, Hansson GK, Nordström P. Osteoprotegerin promotes fibrous cap formation in atherosclerotic lesions of ApoE-deficient mice—brief report. *Arterioscler Thromb Vasc Biol*. 2009;29:1478–1480. doi: 10.1161/ATVBAHA.109.188185
 51. Candido R, Toffoli B, Corallini F, Bernardi S, Zella D, Voltan R, Grill V, Celeghini C, Fabris B. Human full-length osteoprotegerin induces the proliferation of rodent vascular smooth muscle cells both in vitro and in vivo. *J Vasc Res*. 2010;47:252–261. doi: 10.1159/000257339
 52. Toffoli B, Pickering RJ, Tsorotes D, Wang B, Bernardi S, Kantharidis P, Fabris B, Zauli G, Secchiero P, Thomas MC. Osteoprotegerin promotes vascular fibrosis via a TGF- β 1 autocrine loop. *Atherosclerosis*. 2011;218:61–68. doi: 10.1016/j.atherosclerosis.2011.05.019
 53. Moran CS, Jose RJ, Biros E, Golledge J. Osteoprotegerin deficiency limits angiotensin II-induced aortic dilatation and rupture in the apolipoprotein E-knockout mouse. *Arterioscler Thromb Vasc Biol*. 2014;34:2609–2616. doi: 10.1161/ATVBAHA.114.304587
 54. Bumdelger B, Kokubo H, Kamata R, Fujii M, Yoshimura K, Aoki H, Orita Y, Ishida T, Ohtaki M, Nagao M, et al. Osteoprotegerin prevents development of abdominal aortic aneurysms. *PLoS One*. 2016;11:e0147088. doi: 10.1371/journal.pone.0147088
 55. Vorkapic E, Kunath A, Wågsäter D. Effects of osteoprotegerin/TNFRSF11B in two models of abdominal aortic aneurysms. *Mol Med Rep*. 2018;18:41–48. doi: 10.3892/mmr.2018.8936
 56. Bumdelger B, Otani M, Karasaki K, Sakai C, Ishida M, Kokubo H, Yoshizumi M. Disruption of Osteoprotegerin has complex effects on medial destruction and adventitial fibrosis during mouse abdominal aortic aneurysm formation. *PLoS One*. 2020;15:e0235553. doi: 10.1371/journal.pone.0235553

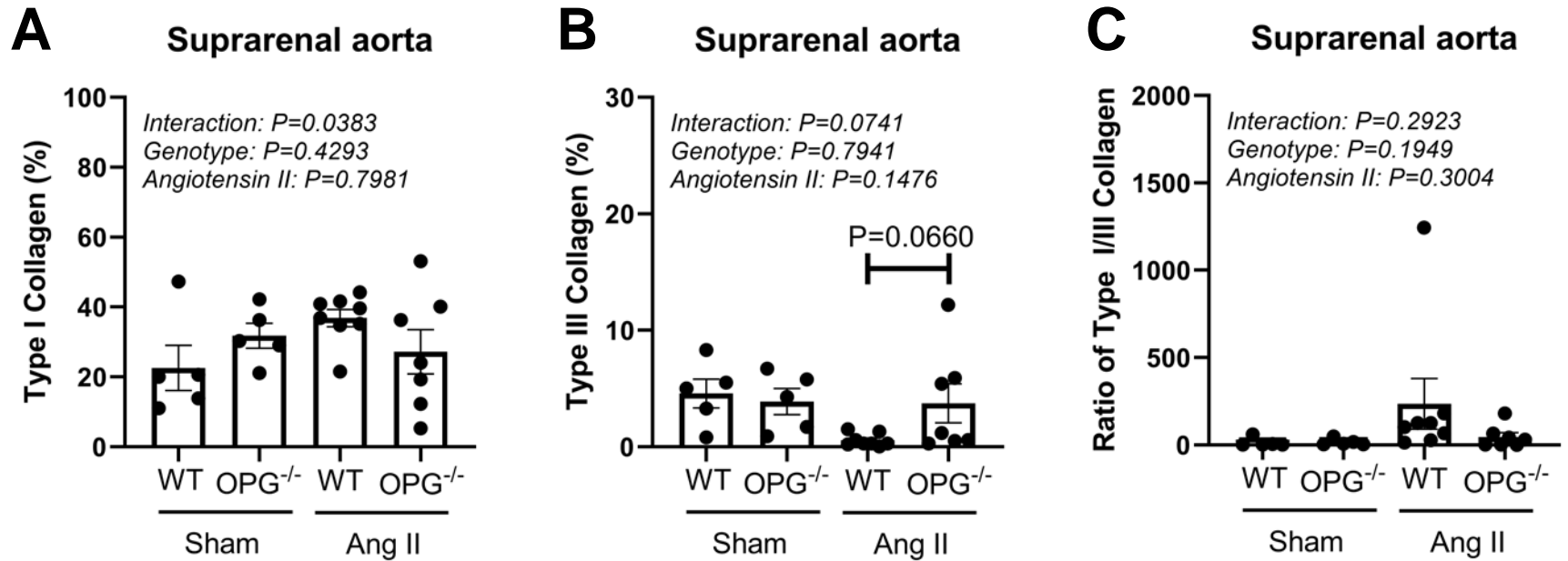
SUPPLEMENTAL MATERIAL

Figure S1.



The immunoreactivity for OPG at the sites of aortic arch (A, E), thoracic aorta (B, F), supra-renal aorta (C, G), and abdominal aorta (D, H) in aortic cross-sections in 2 wild-type mice (A-D, E-H) administered angiotensin II for 28 days. Bar, 200 μ m

Figure S2.



Aortic sections stained with picosirius red were scanned ($200\times$ magnification) using the BX43 microscope (Olympus, Tokyo, Japan) exposed to polarized light with identical exposure time (800 msec) and sensitivity (ISO400) (cellSens Imaging Software. ver.3.1) (Olympus, Tokyo, Japan). **A**, percentage of type I (yellow) and **B**, type III (green) collagens occupied in the adventitia were calculated with identical threshold (WinRoof2018, Mitani Co. Tokyo, Japan). **C**, ratio of type I/III collagen was defined as the percentage of type I collagen divided by type III collagen. Data are presented as means \pm SEM (Sham: WT, $n = 5$, OPG^{-/-}, $n = 5$; Ang II: WT, $n = 8$, OPG^{-/-}, $n = 7$).